PCCP

Accepted Manuscript

This is an *Accepted Manuscript*, which has been through the Royal Society of Chemistry peer review process and has been accepted for publication.

Accepted Manuscripts are published online shortly after acceptance, before technical editing, formatting and proof reading. Using this free service, authors can make their results available to the community, in citable form, before we publish the edited article. We will replace this *Accepted Manuscript* with the edited and formatted *Advance Article* as soon as it is available.

You can find more information about *Accepted Manuscripts* in the **Information for Authors**.

ROYAL SOCIETY
OF CHEMISTRY

www.rsc.org/pccp

Reaction Dynamics Inside Superfluid Helium Nanodroplets. The Formation of the Ne₂ Molecule From Ne + Ne@(^{4}He)$_N$

Arnau Vilà and Miguel González*

Departament de Química Física i IQTC, Universitat de Barcelona, c/ Martí i Franquès, 1, 08028 Barcelona, Spain.

Abstract

The hybrid time dependent quantum dynamics approach [DFT (helium) + quantum wave packet (dopant)] proposed by us (*J. Chem. Theory Comput.*, **2015**, 11, 899-90) has been extended to consider bimolecular type reactive processes involving a superfluid helium nanodroplet [A + B@^{4}He$_N$ $\rightarrow$ AB@^{4}He$_{N'}$ + (N-N')^{4}He, with A and B being atomic species]; T=0.37 K. This is probably the first theoretical attempt to study the reaction dynamics of this kind of processes and in this initial investigation the total angular momentum has been taken as zero. The Ne + Ne@^{4}He$_N$ $\rightarrow$ Ne$_2$(v=0)@^{4}He$_{N'}$ + (N-N')^{4}He reaction has been considered as the first application example and we have examined the influence of different nanodroplet sizes (N=200, 500 and 1000) and initial velocities of the outer Ne atom ($<v_0>$=120-1000 m/s) on the dynamics. The inner Ne atom only produces a greater reduction of the velocity of the outer Ne atom in comparison to what happens in the case of the capture of a Ne atom by a pure nanodroplet. The formation of the Ne$_2$ molecule is a complex phenomenon related with the nature of the helium density waves produced and their reflection from the nanodroplet surface. Though the effective potential energy of Ne$_2$ in the nanodroplet is very different from the gas phase case, the equilibrium Ne-Ne distance is only slightly reduced with respect to the gas phase value, and its vibrational wave function (v=0) is only modified by a 15% with respect to the gas phase one. Furthermore, the analysis of experiments on the capture of Ar, Kr and Xe with larger nanodroplets suggests that the amount of evaporated

helium atoms obtained here is too low for initial velocities above 120 m/s. This problem probably arises from the DFT description of the superfluid helium nanodroplet. We hope that this work will encourage researchers to investigate these very interesting processes on which we still know very little. Lastly, it is worth noting that the quantum treatment presented here can also be applied directly to the study of the photodissociation of an arbitrary diatomic molecule in a superfluid helium nanodroplet.

Keywords: superfluid helium nanodroplet, dopant, Ne atom, Ne_2 diatomic molecule, reaction dynamics, theory, time dependent DFT, time dependent quantum dynamics.

Tables: 2   **Figures:** 9

Supporting Information (see the contents description in page 27)

* Corresponding author: E-mail: miguel.gonzalez@ub.edu; Fax: +34934021231.

1. INTRODUCTION

The study of superfluid helium nanodroplets, ^4He_N (T=0.37 K), is a well-established investigation area in physics.[1,2] They have a large interest as they allow the researchers to achieve a deep insight into the properties of quantum fluids (structure, energy and dynamics), and on how they are modified when the size of the system is changed. Moreover, the nanodroplets can be used as low temperature matrices in high resolution spectroscopic studies, thanks to the chemically inert character of ^4He and its superfluid behavior for T<2.17 K. [3,4,5]

From a chemical perspective,[6,7] these systems constitute genuine nanoreactors, offering the possibility of having a single reactive collision inside them (i.e., only two reactive species are involved in addition to the helium solvent). This can be achieved in the experiments using suitable set up conditions, so that a single species (atom or molecule) is captured by the nanodroplet when it passes along the first pick up chamber, and then a second species is captured in the second chamber.[6,7] The energy transferred to the nanodroplet, coming from both the reactants kinetic energy and the reaction energy involved in the chemical bonds breaking and formation, is easily released by the nanodroplet through the evaporation of some helium atoms (see, e.g., refs 8, 9, 10, 11). Besides, the solvation shells formed around the dopant atoms or molecules are able to stabilize metastable chemical species.

Since the initial study of a chemical reaction in ^4He_N,[12] the contributions reported on the chemical reactivity in ^4He_N have been significant (see, e.g., refs 6, 7, 8, 9, 10, 13, 14 and refs cited there), although the intensity of these efforts is not equivalent to the one dedicated to the research in the physical context. However, the interest of the chemical community on this quantum fluid has augmented in a substantial way in recent times, probably largely due to the new synthetic opportunities offered by ^4He_N; which allows to synthesize chemical species that would not be stable in gas phase (e.g., some metallic nanoclusters[15,16,17] and nanowires[18,19]).

Some attention has also been devoted to the reaction dynamics[1,6] from an experimental perspective (photodissociation of alkyl iodides,[20,21,22] reactions involving metals, Mg + O_2,[23] Al + O_2, H_2O,[14] Ba + N_2O,[12] etc.) and also theoretically (photodissociation of $Cl_2(B)$ in superfluid[8,9,10] and non-superfluid[24] helium nanodroplets). The species produced, of course, can also be regarded as probes for investigating the behavior and properties of liquid helium, considering the widely different types of motions implied in a chemical reaction (i.e., translational, vibrational and rotational motions).

Moreover, the formation of bimetallic clusters in superfluid helium nanodroplets have been analyzed by atomic resolution electron tomography,[25] and the collision times in helium nanodroplets have been studied theoretically for the Cu_2, Ag_2 and Au_2 clusters.[26] Besides, the ^4He droplet-mediated soft-landing deposition of metal nanoparticles on solid surfaces has been investigated experimentally[27,28] (see also refs. 15,16,17,18,19), and the first theoretical evidence of this type of deposition process has been recently provided, considering the collision of $Au@(^4He)_{300}$ with the $TiO_2(110)$ surface (short-time collision dynamics).[29]

We have recently proposed a hybrid quantum dynamics method to investigate the photodissociation dynamics of homonuclear diatomic molecules inside superfluid helium nanodroplets [A_2(ground state)$@(^4He)_{N}$ + hν → A_2(excited state)$@(^4He)_N$ → 2A + $(^4He)_{N'}$ + (N-N')^4He, where the last term simply refers to the total number of evaporated He atoms].[8] In this method the helium is described according to the time dependent density functional theory (TDDFT) and the dopant molecule is described using a wave packet (WP); and this approach was initially applied to analyze the photodissociation of Cl_2 in the B excited state.[8,9,10] To the best of our knowledge this was the first theoretical attempt to study the dynamics of a reactive process in superfluid helium nanodroplets.

Here, we have extended this method to account for the more complex reactive process leading to the formation of a diatomic molecule: A + B$@^4He_N$ → AB$@^4He_{N'}$ + (N-N')^4He, where A

4

and B are atomic species. The present approach can also be employed in a straightforward way to describe the photodissociation of an arbitrary (heteronuclear or homonuclear) diatomic molecule in $^4\text{He}_N$. As a result of the high computational cost required for a quantum description of the reaction dynamics, in this first theoretical study on the formation of a molecule inside a superfluid helium nanodroplet, we have considered the case of zero total angular momentum (head-on collisions).

Quantum effects are expected to be relevant here since we are studying a quantum fluid and also because we are examining the formation of a molecular species. This species has quantized vibrational states that, finally, as a result of the energy exchange with the surrounding helium, will relax to the ground vibrational state. This situation and the processes involved are of quantum nature.

We have selected, as a first example of application, a reaction leading to the formation of a van der Waals (vdW) diatomic molecule and, more concretely, to the production of Ne_2 [Ne + Ne@$^4\text{He}_N \rightarrow \text{Ne}_2$@$^4\text{He}_{N'}$ + $(N-N')^4\text{He}$] with $N=200$, 500 and 1000 and initial expected velocities of the attacking Ne atom, $<v_0>$, in the 120-1000 m/s interval. The quantum dynamics study of the pickup (capture) process of a Ne atom [Ne + $^4\text{He}_N \rightarrow \text{Ne}$@$^4\text{He}_{N'}$ + $(N-N')^4\text{He}$] recently performed by us[11] corresponds to the previous stage to the present study.

The formation of the Ne_2 dimer was studied previously at a DFT level, as a first step for examining the formation of quantum gels by doping liquid helium with many Ne atoms.[30,31] An effective adiabatic potential energy surface (PES) was determined for Ne_2, considering an instantaneous relaxation of liquid helium for each value of the relative distance between the two Ne atoms. Here, our approach to this vdW reaction is completely different, since we have carried out a real-time quantum dynamics study of the process.

The theoretical methods employed are explained in section 2, the most important results achieved are described and analyzed in section 3, the summary and conclusions are presented in

5

section 4, and a Supporting Information (SI) document with useful material (tables, figures and movies) has been included.

2. THEORETICAL METHODS

In the study of a complex system (high number of atoms or degrees of freedom involved), regardless of its nature, mixed or hybrid type theoretical approaches are commonly used ("divide and conquer" strategy). Therefore, a small but very important part of the system is described at a theoretical level substantially higher than the rest of system (see, e.g., refs. 24,32,8,9,29,33). Thus, e.g., in ref. 24 the photodissociation of $Cl_2(B)$ embedded in a non-superfluid helium nanodroplet (T=4 K) was studied, describing the molecule by means of a quantum wave packet and the helium according to the path integral centroid molecular dynamics method.

Once the TDDFT approach was introduced to account for the time evolution of superfluid helium nanodroplets (T<2.17 K), [34] the evolution of the electronic or atomic systems (dopants/impurities) in superfluid helium nanodroplets was studied following a hybrid approach analogous to the one indicated above[24] (TDDFT (helium) + quantum (electron)[32] or classic (atoms)[35]). And more recently this hybrid method was extended to the study of the dynamics of reactive processes (photodissociation of Cl_2 (B)) in helium nanodroplets,[8,9] as well as to the soft-landing deposition of metal nanoparticles, embedded in helium nanodroplets, on solid surfaces.[29]

Here, to investigate the reactive processes occurring inside superfluid helium nanodroplets and involving two atomic species, we have combined one of the main methods employed to describe rather large systems of bosonic liquid helium (TDDFT) and a common method used in gas phase time dependent quantum reaction dynamics to describe the atomic relative motion (quantum wave packet (WP)). We have studied as a first case of application the following process involving the formation of the Ne_2 vdW molecule:

$$Ne(^1S) + Ne(^1S)@^4He_N \rightarrow Ne_2(X^1\Sigma_g^+, v=0, j=0)@^4He_{N'} + (N-N')^4He \qquad (1)$$

6
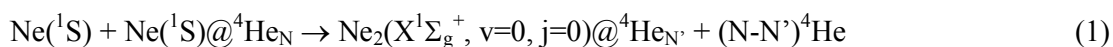
, where the last term refers to the total number of evaporated helium atoms.

This method is an extension of that developed by us for the study of the photodissociation of homonuclear diatomic molecules inside helium nanodroplets,[8,9,10] as previously mentioned. Thanks to the zero total angular momentum approach (head-on collision) the present problem has only five degrees of freedom: three correspond to the helium density and two correspond to the dimer coordinates (Ne-Ne relative and Ne_2 center of mass coordinates).

A quantum description has been used for the helium density coordinates and the Ne-Ne relative coordinate, while classical mechanics has been used for the Ne_2 center of mass (CM) coordinate. This strategy highly reduces the computational cost, compared with treating all the Ne_2 degrees of freedom in a quantum manner, and it is justified by the mass of the effective particles associated to each degree of freedom (the reduced mass, $\mu_{Ne_2} = \frac{m_{Ne}}{2}$, and the total mass, $M_{Ne_2} = 2m_{Ne}$, correspond to the relative and CM coordinates, respectively).

There are two features involved in this theoretical treatment that are mixed together: the coordinates and the physical (quantum *vs*. classical) description. A brief discussion of this issue is important in order to justify the suitability of our choice. Excepting the mean field approximation coming from the DFT description of liquid helium, a full quantum mechanical description of the dimer would imply its total wave function. This wave function could be written, e.g., in terms of the positions of the two Ne atoms or, alternatively, using the relative (Ne-Ne) and center of mass (Ne_2) coordinates. Apart from possible larger or smaller difficulties in the interpretation of the results, depending on the coordinates choice, the selection of coordinates has, of course, no effect on the description of the system.

Some reasonable approximations are needed for computational reasons in order to reduce the complexity of the problem. Within a quantum description of the system, a simplification can be done by factorizing the total wave function of the Ne atoms into two independent wave functions,

each depending on a single degree of freedom. This mean field quantum description of the Ne atoms has the consequence of losing some part of the correlation between them. Instead of this, we have used a quantum description of the Ne-Ne relative coordinate and assumed the CM wave function to be a Dirac's delta function (classical description).

For the purposes of the present work it is more convenient to deal with the relative and CM coordinates than with the coordinates of the two atoms. Focusing in the molecule and regardless of whether the bond is being formed (synthesis) or broken (dissociation), the most natural way to describe it is by means of the relative coordinate; since the separation of the two atoms is what is really important here, no matter where they are placed. This argument is reinforced when focusing on the vibrational motion, which cannot be satisfactorily described using a quantum mean field approach. Furthermore, if we had used atomic position coordinates, although we had treated each Ne atom with a quantum description, i.e., including the zero point energy motion, it would have been less accurate to account for the formation of the molecule.

The superfluid liquid 4-helium has been described using the so-called phenomenological Orsay-Trento (OT) functional[36] where, as usual,[8,9,10,11,35,37,38,39] for computational reasons we have neglected the non-local contributions to the correlation energy and the backflow term. Only recently it has been possible to investigate theoretically the dynamics of chemical and physical processes involving these nanodroplets and atoms or molecules.[8,9,10,11,35,37,38,39] In these studies the approximation of the OT functional indicated above has also been used, due to the computational cost of considering the two terms mentioned above and the major numerical complications arising from the second term. Moreover, when it has been possible to compare the theoretical results achieved using this approximation with the experimental ones, a quite satisfactory agreement has been found;[35,37,39] and some suitable theoretical tests have been reported in the context of the relaxation dynamics of superfluid helium nanodroplets.[10]

The quantum action of the system (eq 2) is written in terms of the effective complex wave function for helium, $\Psi_{He}(\boldsymbol{R}_{He}, t)$, that is defined by $|\Psi_{He}(\boldsymbol{R}_{He}, t)|^2 \equiv \rho_{He}(\boldsymbol{R}_{He}, t)$, the neon atoms relative coordinate wave packet, $\varphi_{rel}(r, t)$, and the neon atoms center of mass coordinate R_{CM}, and is given by

$$
\mathcal{A}[\Psi_{He}, \varphi_{rel}, R_{CM}]
$$

$$
= \int dt \left\{ E[\Psi_{He}, \varphi_{rel}, R_{CM}] - i\hbar \int d\boldsymbol{R}_{He} \, \Psi_{He}^*(\boldsymbol{R}_{He}, t) \frac{\partial}{\partial t} \Psi_{He}(\boldsymbol{R}_{He}, t) \right.
$$

$$
\left. - i\hbar \int dr \, \varphi_{rel}^*(r, t) \frac{\partial}{\partial t} \varphi_{rel}(r, t) - M_{Ne_2} v_{CM}^2 \right\}
$$

$$(2)$$

, where the energy of the system is expressed as

$$
E[\Psi_{He}, \varphi_{rel}, R_{CM}]
$$

$$
= \frac{\hbar^2}{2m_{He}} \int d\boldsymbol{R}_{He} \, |\nabla \Psi_{He}|^2 + \int d\boldsymbol{R}_{He} \, \mathcal{E}_c[\rho_{He}]
$$

$$
+ \int d\boldsymbol{R}_{He} \int dr \, V_{He-Ne_2}(r, \boldsymbol{R}_{He}, R_{CM}) \, \rho_{He}(\boldsymbol{R}_{He}, t) |\varphi_{rel}(r, t)|^2
$$

$$
- \frac{\hbar^2}{2\mu_{Ne_2}} \int dr \, \varphi_{rel}^*(r, t) \frac{\partial^2}{\partial r^2} \varphi_{rel}(r, t) + \int dr \, V_{Ne_2}(r) \, |\varphi_{rel}(r, t)|^2 + \frac{1}{2} M_{Ne_2} v_{CM}^2
$$

$$(3)$$

Regarding the interaction energy potentials, we have followed the common pairwise strategy, expressing the V_{He-Ne_2} potential energy as a sum of the two corresponding two-body V_{He-Ne} terms. Both the V_{He-Ne} and V_{Ne_2} potential energy terms have been taken from ref 40.

In order to determine the set of coupled equations of motion governing the evolution of each degree of freedom, a minimization of the quantum action with respect to $\Psi_{He}(\boldsymbol{R}_{He}, t)$, $\varphi_{rel}(r, t)$, and R_{CM} has to be made, and we have obtained the following expressions:

$$i\hbar \frac{\partial}{\partial t} \Psi_{He}(\boldsymbol{R}_{He}, t)$$

$$= \left[-\frac{\hbar^2}{2m_{He}} \boldsymbol{\nabla}^2 + \int dr\, V_{He-Ne_2}(r, \boldsymbol{R}_{He}, R_{CM}) \, |\varphi_{rel}(r,t)|^2 + \frac{\delta \mathcal{E}_c[\rho_{He}]}{\delta \rho_{He}} \right] \Psi_{He}(\boldsymbol{R}_{He}, t)$$

$$i\hbar \frac{\partial}{\partial t} \varphi_{rel}(r,t) = \left[-\frac{\hbar^2}{2\mu_{Ne_2}} \frac{\partial^2}{\partial r^2} + V_{Ne_2}(r) + \int d\boldsymbol{R}_{He} V_{He-Ne_2}(r, \boldsymbol{R}_{He}, R_{CM}) \rho_{He}(\boldsymbol{R}_{He}, t) \right] \varphi_{rel}(r,t)$$

$$M_{Ne_2} \frac{d^2 R_{CM}}{dt^2} = -\frac{\partial}{\partial R_{CM}} \int d\boldsymbol{R}_{He} \int dr\, V_{He-Ne_2}(r, \boldsymbol{R}_{He}, R_{CM}) \, \rho_{He}(\boldsymbol{R}_{He}, t) |\varphi_{rel}(r,t)|^2$$

(4a, 4b and 4c)

where $\rho_{He}(\boldsymbol{R}_{He}, t)$ and $\mathcal{E}_c[\rho_{He}]$ are the density and correlation energy density of liquid ^{4}He, respectively. $\mathcal{E}_c[\rho_{He}]$ takes into account the potential and strong correlation energies between the He atoms in the superfluid state. Eqs 4a and 4b are the Schrödinger-like non-linear time dependent equations for the helium and Ne-Ne relative motions, respectively, and eq 4c is the Newton equation for the Ne$_2$ CM motion.

A discretization of the space in a grid of points for the degrees of freedom involved has been performed for solving eqs 4a and 4b (Table S1 (SI)). The derivative with respect to the CM coordinate (eq 4c) has been calculated using the chain rule, taking advantage of the analytical function available for the V_{He-Ne_2} potential energy. The time evolution has been calculated numerically by means of a fourth order Adams predictor-corrector-modifier method,[41] that has been initiated by a fourth order Runge-Kutta method,[42] and the time step used is equal to 1.0×10^{-4} ps. The derivatives for the kinetic energy terms in eqs 4a and 4b have been calculated in momentum space, employing a Fourier transform as implemented in the FFTW package of ref 43.

Moreover, a quartic negative imaginary potential (NIP)[44] has been placed at the edges of the helium Cartesian grid, in order to absorb the helium density evaporated from the nanodroplet and avoid artificial reflections. The NIPs have the following expression:

$$V_{\text{NIP}} = -i A \frac{5}{2} \left(\frac{d - d_{\text{NIP}}}{L} \right)^4$$

<div align="right">(5)</div>

for $d > d_{\text{NIP}}$, where the absorption strength (A) is equal to 3315.0 K Å^{-4}, the length (L) is equal to 1.0 Å, and the NIPs are located (d_{NIP}) 1.0 Å before the grid limits (x_{max}, y_{max}, z_{max}); cf. in Table S1 the data for N=500 (nanodroplet radius = 20.0 Å).

We now focus on the initial conditions explored in the study of the reaction dynamics. Several Ne@^{4}He$_N$ doped nanodroplets (N = 200, 500 and 1000, where a particularly detailed analysis is provided for N = 500) and average initial velocities of the impinging Ne atom (120-1000 m/s interval) have been considered. This atom has been always located initially far enough from the nanodroplet where, essentially, no interaction is present (Table S1).

The theoretical treatment (zero total angular momentum) restricts the diatomic problem to a single dimension problem (molecular axis = z axis), and the initial time static (ground state) calculation of the doped nanodroplet Ne@^{4}He$_N$ must be consistent with it. Thus, in the initial static nanodroplet the Ne impurity has been treated quantum mechanically in the z-axis motion, with its wave function (wave packet) and the corresponding zero point energy motion, and has been treated classically in the x- and y-axis motions (i.e., simply acting as an external potential). Of course, this introduces a small anisotropy in the nanodroplet density (Figure 1). However, if the initial static nanodroplet were computed considering the full Ne atom wave function, the nanodroplet would start its motion without the external boost caused by the impinging Ne atom; due to the different treatments of the impurity considered in the static calculation (initial time for the dynamics) and in the dynamics study. The numerically obtained z-axis wave function has been then fitted to a Gaussian function to be used in a suitable way to define the initial condition for the dynamics, where different grids have been employed, depending on the initial velocity (Table S1).

Furthermore, when changing from the initial time (static result) to the dynamic calculation,

the initial wave packet describing the relative coordinate of the Ne atoms must be consistent with the corresponding "translational" wave function of the inner Ne atom. To do this we have taken into account the meaning of the probability density of a quantum wave function. Once the mean value of the initial position of both Ne atoms has been defined, we have deduced $R_{CM,t=0}$ and $\langle r \rangle_{t=0}$. Thus, scanning the different possible values of the relative coordinate (grid values) leads to the corresponding values of the inner Ne atom position (eq 6a). Then, we have associated a probability to each configuration by means of the "translational" wave function $\phi_{Ne\ inner}(z)$ coming from the (ground state) static calculation of the doped nanodroplet (eq 6b):

$$z(r_i) = R_{CM,t=0} + \frac{1}{2} r_i \qquad \forall r_i \in grid\,[r_{min}, r_{max}]$$

$$\rho_{rel}(r_i) = \left| \phi_{Ne\ inner}(z(r_i)) \right|^2$$

$$\text{(6a and 6b)}$$

This is the way we have followed to define the initial (t=0) relative coordinate wave packet probability density. Finally, a boost operator is applied to this wave function to obtain the corresponding initial relative velocity, which is easily obtained from a change of coordinates:

$$\varphi_{rel}(r_i) = \sqrt{\rho_{rel}(r_i)}\, exp\left\{ i \frac{\mu_{Ne_2} v_{rel,t=0}}{\hbar} r_i \right\}$$

$$\text{(7)}$$

3. RESULTS AND DISCUSSION

The formation of the van der Waals diatomics Ne_2 inside helium nanodroplets has been studied for the $Ne + Ne@(^4He)_N$ reaction considering different initial velocities of the impinging Ne atom. The velocities have been selected taking into account the Maxwell velocity distribution of Ne at room temperature (typical experimental conditions; see Figure S1 (SI)), in order to investigate the influence of the velocity on the reaction dynamics (reaction mechanism and other properties). The six cases studied in particular detail correspond to the initial average velocities $\langle v_0 \rangle$ = 120, 300, 500, 750, 800 and 1000 m/s (where 500 m/s corresponds to the most probable value at 300 K) and

the nanodroplet of 500 ^{4}He atoms; of course, we are considering "initial average velocities" as the relative motion of the two Ne atoms is described quantum mechanically. The effect of the nanodroplet size on the microscopic reaction mechanism has been also investigated. Thus, some representative initial velocities have been chosen ($<v_0>$ = 120, 300 and 800 m/s) for nanodroplets of 200 and 1000 helium atoms.

In order to understand better the microscopic mechanism of this reaction some movies corresponding to N=500 and three initial velocities (120, 500 and 800 m/s) are given in the Supporting Information (Movies 1-3). Besides, in Figure 2 it can be seen the evolution of the helium density along the z-axis (molecular axis) for the reactive process at $<v_0>$ = 300 m/s and $N =$ 500. The first reaction step for the formation of the van der Waals dimer consists in the pickup of the impinging neon atom by the neon-doped helium nanodroplet. This process resembles the pickup of a Ne atom by a helium nanodroplet studied before,[11] but it has some peculiarities owing to the presence of the dopant Ne atom inside the nanodroplet.

From Figure 2 it can be seen that once the attacking Ne atom collides with the nanodroplet surface ($t \approx 2.3$ ps) the nanodroplet is compressed and helium density waves are produced. Then, the atom overcomes the surface tension and generates a dimple in the vicinity of the nanodroplet surface which is subsequently closed ($t \approx 6.9$ ps) placing the atom inside the nanodroplet and, therefore, leading to the capture. This atom continues moving inside the nanodroplet and producing the compression of helium, until there comes a time when, as a result of the fusion of the solvation shells of both Ne atoms, a peak of high helium density separating the two atoms is generated ($t \approx$ 19.0 ps). This corresponds to the last obstacle for the reaction to occur and, until this moment, the location of the internal Ne atom has changed very little from its initial position in the center of the nanodroplet (x = y = z = 0). After some time, this peak of density disappears allowing the formation of the Ne$_2$ dimer. The times corresponding to different nanodroplet sizes and initial velocities and also some specificities can be seen in Movies 1-7 (SI).

It is worth noting that in the theoretical framework adopted here the possibility to account for the partial penetration of the impinging atom into the nanodroplet cannot be described. The wave function employed in our investigation describes the Ne-Ne relative distance degree of freedom. So that, this makes the wave function always confined by the potential, because there is always a Ne atom placed inside the nanodroplet. Therefore, keeping the center of mass constant at a certain value, when varying the value of the relative coordinate, the inner atom approaches to the walls of the helium bubble and, hence, the potential becomes repulsive. This fact, however, does not represent a problem for the theoretical description of the reaction at the selected initial velocities, as we know that Ne atom capture probability by $(^4He)_{1000}$ is equal to one for these initial velocities (for $<v_0> = 120$ m/s the capture probability is really equal to 0.99).[11] From our model it comes out that if capture takes place this will lead necessarily to reaction.

The previous reasoning supports the idea that the present theoretical model is satisfactory for the description of the reactive process we are interested in. Besides, although two wave packets (two translational wave functions, one for each Ne atom) could also be used to describe the reaction, the approach employed here, based on the relative coordinate wave packet and the classical treatment of the Ne_2 center of mass motion, allow us to account in a more natural way for the formation of the Ne_2 molecule.

The examination of the movies shows the existence of another important difference when comparing the reactive process occurring in the doped nanodroplet with the capture process taking place in a pure nanodroplet:[11] the high reduction of the impinging Ne atom velocity due to the presence of the inner Ne atom. This can even produce the rebound (negative velocities) of the former Ne atom. To clarify this effect we have estimated the expected position of each neon atom (A and B) by:

$$z_{Ne\binom{A}{B}} = R_{CM} \pm \frac{1}{2}\langle r \rangle$$

(8)

, where A and B refer to the inner and impinging neon atoms, respectively.

The time evolution of these values and the corresponding velocities are plotted in Figure 3. The solid and dashed lines correspond to the estimated positions of the impinging and the inner Ne atoms, respectively. The rebound effect is present for all the main initial velocities studied, with the only exception of the lowest one ($<v_0> = 120$ m/s). A detailed visualization of the Movies 1-3 (SI) points out that this can be caused by different reasons, depending on the case. For low initial velocities this is probably mainly due to the reflection of the helium shock waves initially generated by the impinging Ne atom, while for high initial velocities this probably results from the huge compression of the helium density between the two Ne atoms.

The trajectory of the mean values of the Ne atoms velocities and positions are given in Figure S2. The results for the impinging Ne atom are similar to what has been found for the pick up process in a pure nanodroplet,[11] but important oscillations are observed in the velocity for the present case when this atom is inside the nanodroplet. This happens due to the presence of the inner Ne atom.

Focusing now on the formation of the vdW molecule, it can be inferred that the mechanism of this process is not unique, but depends on the initial situation. For the nanodroplet with $N = 500$ [4]He atoms we have found that in all cases the Ne_2 molecule is produced close to the center of the nanodroplet, except for $<v_0> = 500$ m/s. In this case the Ne atoms move through the nanodroplet at a fairly constant separation between them until they get close to the surface, where the molecule is formed. This happens because the microscopic reaction mechanism depends on the effectiveness of the momentum transfer from the impinging neon atom to the inner one, which is mediated by the liquid helium. This is a complex process involving several degrees of freedom, the density waves generated and their interferences. Hence, for a given nanodroplet there is a non-monotonic relationship between the initial velocity and the mechanism. This is also supported from the

analysis of the nanodroplet size effect since, for a given initial velocity, several mechanisms are found, depending on the size (cf. Movies 1-7 (SI)).

From a structural point of view the formation of the Ne_2 dimer could be considered to occur at the time when the $<r>$ value crosses for the first time the asymptotic $<r>$ value (expected value of the $Ne_2(v=0)$ distance in the nanodroplet; cf. Figure 4). After that, the dimer is just relaxing, i.e., releasing its excess of energy. Alternatively, from the energy perspective the van der Waals molecule can be considered as formed when the two atoms are in a bound state, i.e., when the expected value of the total relative coordinate energy ($\langle E_{total,\ rel} \rangle \equiv \langle E_{pot\ Ne-Ne} \rangle + \langle E_{kin\ rel} \rangle$) is negative. The time evolution of $\langle E_{total,\ rel} \rangle$ as a function of the initial velocity is plotted in Figure 5. From this figure and Figure 4 it comes out that these two ways to define the formation of Ne_2 lead to essentially the same result as, in fact, the structural and energy conditions are almost equivalent. Then, we estimate a time scale of about 17-43 ps for the formation of this molecule, depending on the initial velocity (cf. Table 1).

Moreover, once the van der Waals diatomics is formed inside the nanodroplet, a vibrational relaxation process takes place from states that correspond to superposition of vibrational states, which evolve in a rather fast way into the ground vibrational state ($v=0$) of Ne_2. Thus, this process lasts until the relative coordinate wave packet is transformed into the ground vibrational wave function of Ne_2 in the nanodroplet; which correlates with the oscillations observed in the $<r>$ *vs* time dependence around its asymptotic value (Figure 4) and has a time scale of around 3.5 ps. The pattern of the vibrational relaxation of the molecule mediated by the helium nanodroplet is very similar in all cases. This shows that this process is not highly influenced by the slight differences in the excitation of the nanodroplets.

For times above ≈5 ps the velocity of both Ne atoms is, in general, below the Landau's critical velocity, with the exception of what happens at the beginning of the relaxation of Ne_2 into

the vibrational ground state (Figure 3). The velocity of the incoming Ne atom is reduced in this important way due to the helium, which is energetically excited, as a result of the collision with this atom. The interaction potential of the Ne atoms with the helium clearly dominates (Ne-Ne interaction potential almost negligible) until the helium density placed between the two Ne atoms disappears, allowing the final approach of both atoms (cf. Figure 2). From this moment the Ne-Ne interaction potential is playing a role, even though the Ne_2-helium interaction is stronger than the former one. Furthermore, it is important to note that the finite size character of the system is more evident here (cf. reported results for $(^4He)_{500}$) than for the nanodroplet considered in the pick up process, $(^4He)_{1000}$.[11] Another important feature displayed in Figure 4 is that once the van der Waals molecule is formed it is never broken again.

It should be mentioned that the experimental value of the critical velocity is ≈58 m/s (0.58 Å/ps) in superfluid (bulk) helium[45,46] but the theoretical value is ≈90 m/s.[37] As it was already indicated in section 2, given the great complexity of these systems, the theoretical study of the dynamics has only been possible very recently; being necessary to consider an approximate OT functional (whose main effect is to modify the value of the Landau's critical velocity). However, when it has been possible to compare the theoretical results, determined at this level of approximation, with the experimental results on other properties, a rather good agreement has been obtained;[35,37,39] and some theoretical tests have also been reported.[10] In this context it is also worth noting that currently there are no other theoretical methods available for studying the dynamics of these interesting systems.

During the vibrational relaxation the energy flux between the molecule and the nanodroplet is not monotonic, but the energy is exchanged back and forth between them (Figure 5); although, of course, the excitation energy of the Ne + Ne system above the ground vibrational state ($v=0$) of Ne_2 is completely transferred to the helium. The main amount of energy transferred from the molecule to the nanodroplet occurs at about 1 ps after the total relative coordinate energy reaches the zero

17

value for the first time; and a careful examination of the movies (SI) shows that this is mediated by the emission of a helium density wave of high amplitude.

To deepen into the dynamics of this process, the different contributions to the total relative coordinate energy together with the evolution of $<r>$, for $N=500$ and $<v_0>=120$ m/s, are plotted in Figure 6. Besides, in a static calculation we have also determined the ground state of the doped nanodroplet, $Ne_2(v=0)@^4He_{500}$, in which both the helium density and the vibrational wave function $(\varphi_{Ne_2(v=0)@\ ^4He_{500}}(r))$ are optimized. This allowed us to compute the time evolution of the projection of the Ne_2 vibrational wave function, as the reaction progresses, with respect to the vibrational ground state of Ne_2, i.e., $\left|\left\langle\varphi_{rel}\middle|\varphi_{Ne_2(v=0)@\ ^4He_{500}}\right\rangle\right|^2(t)$, which is also presented in Figure 6 (red line). From this figure it is evident that φ_{rel} evolves progressively into $\varphi_{Ne_2(v=0)@\ ^4He_{500}}$, being both wave functions almost coincident for $t > 38$ ps.

For $N=500$ and $<v_0>=120$ m/s, when $<r>$ is small enough and the wave packet enters into the Ne-Ne potential energy minimum (time ≈ 33 ps; Table 1) the total relative energy remains almost constant, but with an increase and a decrease of the kinetic and Ne-Ne potential energies, respectively; which is analogous to the classical behavior (Figure 6). However, when $<r>$ reaches the first minimum value ("inner turning point" of the Ne-Ne potential energy curve; time ≈ 33.5 ps), the kinetic energy is only slightly reduced. Therefore, this contribution is associated to the kinetic energy part of the zero point energy (ZPE), i.e., related to the width of the wave packet in momentum space, instead of to the relative translational energy. The subsequent fast reduction of the dimer energy found correlates with the re-increase of the $<r>$ value (time interval of 33.5 to 34.3 ps, approximately), i.e., when the Ne atoms of the dimer are separating from each other, pushing the surrounding liquid helium and generating a helium density wave. This process correlates with the reduction of the zero point kinetic energy of Ne_2, i.e., with the narrowing of the wave packet in momentum space (Figure S3 (SI)).

After the emission of the density wave, the vibrational relaxation continues but in a slower way, with some energy exchanges occurring in the two directions. At the end, very small oscillations in the $<r>$ value are present, reflecting the slight changes that happen in the effective potential energy (Ne-Ne and Ne_2-helium potential energies) governing the evolution of the relative distance degree of freedom.

Now, it is worth focusing the attention on the nature of the van der Waals product molecule, as well as on the influence of the helium environment. For the related generic processes $A + A \rightarrow A_2$ and $A + B \rightarrow AB$ in $(^4He)_N$ involving the formation of pure chemical bonds, due to the much higher bond energies implied, we expect that helium will not modify in a substantial way the properties of the product molecule, in comparison to its gas phase properties. In the present case, however, the Ne-Ne dimer vdW interaction (well depth of 41.16 K)[40] is of the same order of magnitude as the Ne-He vdW interaction (well depth of 21.02 K).[40] This fact together with the large number of helium atoms forming the nanodroplet lead to a rather important influence of helium on the properties of Ne_2.

A value of $<r>$ =3.29 Å has been determined for the neon molecule in the $Ne_2@(^4He)_{500}$ doped nanodroplet in the ground state equilibrium configuration, and for long propagation times the evolution of $<r>$ is slightly oscillating around this equilibrium value (cf. Figure 4; dashed line showing $<r>$=3.29 Å). Furthermore, the $<r>$ value for the vibrational ground state ($v=0$) of Ne_2 in gas phase is 3.34 Å. The $<r>$ values are larger than the 3.0988 Å equilibrium Ne_2 distance in gas phase,[40] which is also very similar to the equilibrium Ne_2 distance obtained here from the effective potential of Ne_2 in the nanodroplet.[40] To appreciate in a more clear way the effect of the solvent on the structure of the Ne_2 vdW molecule, the potential energy terms that influence the relative coordinate degree of freedom in the nanodroplet (V_{Ne-Ne} and $V_{Ne2-helium}$) and in the gas phase (V_{Ne-Ne}) and the corresponding vibrational ground state $Ne_2(v=0)$ wave functions are plotted in Figure 7.

The liquid helium leads to a much deeper potential energy curve for the relative coordinate

than in the gas phase. However, although the effective potential energy curve of Ne_2 arising from

the Ne-Ne + Ne_2-helium interactions (V_{eff,Ne_2}) is largely different from the gas phase one,

$$V_{eff,Ne_2}(r) = V_{Ne_2}(r) + \int dR_{He}V_{He-Ne_2}(r, R_{He}, R_{CM} = 0)\rho_{He}(R_{He})$$

(9)

(where, of course, here we are considering the doped nanodroplet in the ground state), the

position of the global Ne_2 minimum is very similar to the gas phase result (only a slight reduction of

the Ne-Ne bond distance occurs). Then, we can conclude that regarding the Ne-Ne interatomic

distance the helium environment only compresses a little bit the Ne_2 dimer bond (Figure 7). This

probably results from a rather complex energy balance involving the Ne-Ne and Ne_2-helium

potential energies and the surface energy (that is related to the helium surface tension) of the walls

of the cavity generated by the molecule in the nanodroplet. Furthermore, the overlap between the

nanodroplet and the gas phase Ne_2 vibrational ground state (v=0) wave functions is equal to 85%.

We should remember that these results correspond to a van der Waals molecule. For a molecule

showing a chemical bond the situation can be very different, as indicated above.

Besides, the energy analysis shows that the nanodroplet Ne_2 wave function(v=0) for N=500

has 2.63 K more of total relative energy (kinetic relative + Ne-Ne potential energies) than the gas

phase one (Table 2). The compression of the dimer induced by the nanodroplet results in a lower

Ne-Ne potential energy (decrease of 1.61 K) but a higher relative kinetic energy (increase of 4.25

K). The difference between the total relative energies is fully compensated by the Ne_2-helium

interaction potential energy, which has attractive character and takes a value of around -244 K.

To conclude this analysis centered in the main results obtained here from the perspective of

the formation of the Ne_2 molecule, we consider an introductory exploration on the effect of the

nanodroplet size on this reactive process. Thus, we have also investigated this reaction for nanodroplets of 200 and 1000 ^{4}He atoms and the initial impinging velocities of 120 and 800 m/s. For $N=200$ the molecule is always formed by a "direct" microscopic mechanism, i.e., the two Ne atoms are always getting closer until the Ne_2 dimer is produced (Movies 4 and 5). The small size of this nanodroplet does not allow other possibilities.

For $N=1000$ and $<v_0>=120$ m/s the Ne_2 is formed near the center of the nanodroplet (Movie 6), while for $<v_0>=800$ m/s the mechanism is more complex. Thus, the high helium density oscillations produced by the impact of the impinging Ne atom with the nanodroplet originates the motion of the inner Ne atom; and due to this the dimer is not formed until the inner atom collides with the nanodroplet surface and rebounds from it (Movie 7). These results reinforce the idea of the complexity of the mechanism for the formation of vdW molecules, which shows no monotonic tendencies. Moreover, it is worth noting that for $N=200$ the nanodroplet suffers strong shape deformations that do not happen for $N=1000$.

In this work, which has been mainly focused on the reaction leading to the formation of Ne_2, the helium nanodroplet has been also considered. We have analyzed the time evolution of the energy per helium atom of the nanodroplet (E/N) and the number of helium atoms (N), which are shown in Figures 8 and 9, respectively. Moreover, the E/N value when Ne_2 molecule is formed is compiled in Table 1 for each selected initial velocity. The results are similar to those obtained for the pickup of a Ne atom by a pure nanodroplet.[11]

For each of the various initial velocities examined, in the case of the Ne_2 dimer formation the maximum value of E/N and the percentage of helium atoms evaporated from the nanodroplet reach values which are twice the ones obtained for the pickup of a Ne atom. This can be explained simply taking into account that the number of helium atoms involved in the study of the reaction ($N = 500$) is half the number of helium atoms considered in the pick up process ($N = 1000$).[11] The expected higher E/N and percentage of evaporated atoms observed when the size of the nanodroplet

decreases has also been found in the theoretical study of the photodissociation of the $Cl_2(B)$ molecule embedded in superfluid helium nanodroplets.[8,9,10]

No significant changes are observed in the time evolution of E/N and N once the Ne_2 vdW molecule has been formed (only a tiny increase in E/N takes place; cf. Figure 8). The situation, of course, would be very different for the formation of a molecule involving a chemical bond (bonding energy ~ electron-volts), due to the large amount of energy that would be released to the nanodroplet. This would lead to a second and important source for the evaporation of helium atoms.

Now, we will consider in a more detailed way the evolution of E/N and N (Figures 8 and 9). When the impinging Ne atom is very close to the surface of the nanodroplet a strong energy transfer begins to occur from the atom to the nanodroplet (E/N initial $(Ne@(^4He)_{500})$ = -4.85 K, which is close to the value obtained for $Ne_2(v=0)@(^4He)_{500}$, -4.75 K, due to the small effect caused by the second Ne atom).

After a certain time and with the attacking atom located deep inside the nanodroplet (z in the range ≈ -7 / -10 Å for 1000-500 m/s) the maximum degree of excitation is reached. This leads to the presence of an intense peak, $(E/N)_{max}$, as it can be seen in Figure 8. The dependence of E/N on time is different for $<v_0>$ = 300 m/s, that shows two maxima of similar intensities (z ≈ -13 / -14 Å), and for $<v_0>$ = 120 m/s, that presents an initial plateau that is followed by second plateau with a higher E/N value (z ≈ -16 Å). Once this E/N maximum has been reached (or the most intense peak and the beginning of the second plateau in the case of 300 and 120 m/s, respectively) the evaporation of the helium atoms begins, which leads to a decrease of E/N with time.

For $<v_0>$ = 500, 750, 800 and 1000 m/s the times required for the maximum degree of excitation to be halved are 10.1, 4.7, 4.4 and 2.9 ps respectively (z ≈ -4 / -6 Å), while the number of helium atoms evaporated are 3.0, 2.6, 2.6 and 2.2, respectively (the numbers are not necessarily integers because is the helium density what is evaporating). And after increases of 26.7, 8.2, 10.4 and 10.3 ps, respectively, the formation of the Ne_2 vdW molecule takes place. Once the Ne_2 species

is formed it moves inside the nanodroplet bouncing a large number of times on the nanodroplet surface. This situation resembles to the rebounds experienced by the Ne atom after its capture by a pure nanodroplet, $(^4\text{He})_{1000}$.[11]

The "asymptotic" limit value of E/N obtained in the longer simulations (120, 500 and 1000 m/s; 78.3, 90.6 and 110.0 ps, respectively) is in the range -4.63 / -4.66 K (Figure 8). These values are not far from that obtained for the doped nanodroplet in the ground state, $\text{Ne}_2(v=0)@(^4\text{He})_{500}$ (-4.75 K; this value changes very little as a result of the evaporation of a few helium atoms). Also noteworthy is that the number of evaporated atoms in the longer simulations is equal to 3, 9 and 14, respectively (Figure 9), i.e., the percentage of evaporated atoms is really small (0.6, 1.8 and 2.8%, respectively).

At this point it is worth completing this analysis by considering qualitatively the possible effect of the inclusion of the angular momentum, the classical description of the neon atoms motion and also to reflect on the number of evaporated atoms determined experimentally for other systems, that it is quite higher than the values found here.[47,48] Unfortunately, there is no experimental data available to compare with for the $\text{Ne} + \text{Ne}@(^4\text{He})_{500}$ reaction.

Regarding the influence of angular momentum, it is expected that the interaction between the attacking neon atom and the nanodroplet would be less "strong" and take a little longer to occur. This can be understood by reasoning in classical terms since, for a given initial velocity, there will be a decrease in the radial component of the velocity as the angular momentum increases. The (orbital) angular momentum, that classically is given by $l = \mu \, v_{\text{rel}} \, b$, where μ is the reduced mass, v_{rel} is the relative velocity, and b is the impact parameter (0.990 m_{Ne}, v_0 and $b =0$, respectively, in the present study), will reach a certain maximum value, l_{max}, above which the capture can not take place (and therefore the reaction can not occur), that depends on the velocity.

If the two Ne atoms were described classically the interaction with the nanodroplet would be more "powerful" (stronger energy transfer to the nanodroplet) because, unlike what happens at the

quantum level (in which each atom has a distribution of possible locations, according to its wave function), classically at each simulation time each of the Ne atoms is located in a unique position of the space. This more "powerful" interaction of the atoms with the nanodroplet when the atomic species are treated classically has been reported in ref. 24, although in that case the helium nanodroplets showed no superfluid character ($T = 4$ K).

The number of helium atoms evaporated and the apparent cross sections for capture and subsequent coagulation of atoms and molecules by superfluid helium nanodroplets (the capture of an atom A is followed by sequential captures and reactions inside the nanodroplet: $A + A \rightarrow A_2$, $A + A_2 \rightarrow A_3$, etc.) have been measured in molecular beam experiments ($N > 10^3$).[47,48] Although in these references there are no results for the Ne atom, it is interesting to consider the number of evaporated atoms produced in a single collision between a noble gas atom (Ar, Kr, Xe) and a nanodroplet ($<N> = 2650$). This number is equal to 244 (9.2%), 313 (11.8%) and 560 (21.1%), respectively, for collision energies ($<E_{col}>$) of 87, 139 and 195 meV, where the numbers in parentheses indicate the percentage of evaporated atoms in each case. These percentages are substantially higher than those obtained theoretically for the Ne atom at $<v_0> = 500$, 800 and 1000 m/s ($<E_{col}> = 26.1$, 66.9 and 104.6 meV) in both the capture process ($\approx 0.5\%$)[11] and the reaction leading to the dimer formation ($\approx 1.2\%$), where smaller nanodroplets are considered ($N = 1000$ (capture) and 500 (reaction)).

Furthermore if we estimate the number of evaporated helium atoms on the basis of the kinetic energy of the impinging Ne atom and taking into account the He bulk binding energy as in ref. 47 (7.2 K/atom), the number of evaporated helium atoms for $<v_0> = 120$, 300, 500, 750, 800 and 1000 m/s should be equal to 2, 15, 42, 95, 108 and 169 atoms, respectively. Hence, the amount of evaporated atoms obtained theoretically is too low, with the exception of what happens for 120 m/s. This problem probably results from the DFT approach used to describe the superfluid helium nanodroplet (its continuous nature leads to a much more excitation of the vaporized atoms and due

to this to a much smaller number of vaporized atoms is required). Furthermore, it should also be indicated that some pick up test calculations carried out by us on the Ne + (^{4}He)$_{500}$ system, assuming a classical mechanics description for the Ne atom and without angular momentum restrictions, led to very similar results, independently of the angular momentum (in particular, a very similar amount of evaporated helium atoms was obtained for all angular momentum values explored, i.e., from l=0 to l_{max}).

4. SUMMARY AND CONCLUSIONS

We have extended our recently proposed hybrid theoretical approach [TDDFT (helium) + quantum wave packet (atom or molecule)] to investigate the reaction dynamics of chemical processes involving superfluid helium nanodroplets, ^{4}He$_N$, and atoms or molecules. This has been done here in order to make possible the study of reactive processes of the type A + B@^{4}He$_N$ $\rightarrow$ AB@^{4}He$_{N'}$ + (N-N') ^{4}He, where A and B are atomic species. Besides, this approach can also be used in a straightforward way to investigate the photodissociation of an arbitrary diatomic molecule in a helium nanodroplet.

This is probably the first theoretical attempt to study the dynamics of a reactive process of bimolecular type in superfluid helium nanodroplets, and in this initial investigation the total angular momentum of the system has been taken as equal to zero. Thanks to this the reaction dynamics can be described using five degrees of freedom. We have used a quantum description for the helium density coordinates (x, y, z) and the A-B relative coordinate (r), while the AB center of mass coordinate (z_{CM}) has been described by classical mechanics.

We have considered, as a first example of application, the Ne + Ne@^{4}He$_N$ $\rightarrow$ Ne$_2$(v=0, j=0)@ ^{4}He$_{N'}$ + (N-N')^{4}He reactive process, which involves the formation of the Ne$_2$ van der Waals molecule, taking into account nanodroplets of different sizes (N=200, 500 and 1000) and several initial mean velocities of the impinging Ne atom ($<v_0>$: 120-1000 m/s).

The capture of the impinging Ne atom by the doped nanodroplet is only slightly modified with respect to what happens in the capture of a Ne atom by a pure nanodroplet. The presence of the inner Ne atom in the doped nanodroplet simply produces a higher reduction of the velocity of the former one in comparison to what is observed in a pure nanodroplet.

The microscopic mechanism for the formation of the Ne_2 dimer does not vary in a simple way as a function of the features of the system. Thus, the Ne atoms follow different paths until the vdW dimer is formed, depending on the nanodroplet size and the impinging velocity. This shows that the formation of the molecule is a complex phenomenon that is related to the nature of the helium density waves produced during the collision with the impinging Ne atom (which are related to the initial velocity) and their reflection from the nanodroplet surface (which is related to the nanodroplet size).

Although the effective potential energy of Ne_2 arising from the Ne-Ne and Ne_2-helium interactions is very different from the potential energy of Ne_2 in the gas phase (Ne-Ne interaction only), the expected Ne-Ne distance (3.29 Å) is very similar to the gas phase value (3.34 Å). Thus, as a result of the helium environment, the Ne_2 product molecule is only slightly compressed and its vibrational wave function (v=0) is only modified by a 15% with respect to the gas phase one.

Despite there is no experimental data available for the studied system, the analysis of the experimental results reported for Ar, Kr and Xe with larger nanodroplets suggests that the amount of evaporated atoms for Ne + $Ne@^4He_N$ obtained theoretically is too low for initial velocities above 120 m/s. This drawback probably comes from the DFT approach used to describe the superfluid helium nanodroplet.

The reaction dynamics in superfluid helium nanodroplets of processes leading to the formation of diatomic molecules involving chemical bonds will be considered by our group in the future, using the same theoretical approach developed here. Finally, we hope that this work will

encourage theoreticians and experimentalists to investigate these very interesting processes on which we still know very little.

Supporting Information

Tables: Table S1. Helium and Ne Cartesian grids (N=500). Table S2. Propagation times (N=500). **Figures**: Figure S1. Maxwell velocity distribution of Ne (T=300 K). Figure S2. Trajectories of the mean values of the Ne atoms velocities and positions (N=500). Figure S3. Time evolution of the probability density of the relative coordinate wave packet (N=500 and $\langle v_0 \rangle$=120 m/s). **Movies**: Movie 1. Time evolution of the relative coordinate wave packet and effective potential. Time evolution of the helium density (xz-plane) for N=500, $\langle v_0 \rangle$=120 m/s. Movie 2. As Movie 1 but for N=500, $\langle v_0 \rangle$=500 m/s. Movie 3. As Movie 1 but for N=500, $\langle v_0 \rangle$=800 m/s. Movie 4. As Movie 1 but for N=200, $\langle v_0 \rangle$=120 m/s. Movie 5. As Movie 1 but for N=200, $\langle v_0 \rangle$=800 m/s. Movie 6. As Movie 1 but for N=1000, $\langle v_0 \rangle$=120 m/s. Movie 7. As Movie 1 but for N=1000, $\langle v_0 \rangle$=800 m/s.

Acknowledgements

Tables

Table 1. Ne_2 formation time and energy per ^{4}He atom for the helium nanodroplet with N=500 at several initial average velocities of the impinging Ne atom.

$<v_0>$(m/s)	Ne_2 formation time (ps)	E/N (K)
120	33.2	-4.59
300	28.8	-4.55
500	42.6	-4.57
750	17.0	-4.41
800	18.7	-4.42
1000	16.5	-4.35

Table 2. Energy of the Ne_2 vibrational ground state relative coordinate wave function in gas phase and in the ^{4}He$_{500}$ nanodroplet.

Phase	$E_{kin\ relative}$ (K)	$E_{pot\ Ne-Ne}$ (K)	$E_{total\ relative}$ (K)
Gas	7.46	-30.93	-23.47
^{4}He$_{500}$	11.71	-32.54	-20.84

Figure captions

Figure 1. Helium density profiles in the z (molecular axis), x and y axes for the initial time of the dynamics. The center of the nanodroplet corresponds to the origin of coordinates.

Figure 2. Snapshots showing the time evolution of the helium density along the molecular axis (z axis). The position of the Ne atoms is schematically represented by the purple balls. The initial average velocity of the impinging Ne atom is 300 m/s.

Figure 3. Position (up) and velocity (down) of the impinging (solid line) and inner (dashed line) Ne atoms, as a function of time.

Figure 4. Expected value of the relative coordinate as a function of time. The dashed line corresponds to the asymptotic $<r>$ value (3.29 Å).

Figure 5. Expected value of the total relative energy (kinetic energy + Ne-Ne potential energy), as a function of time. The vertical lines indicate the beginning of the vibrational relaxation process.

Figure 6. Time evolution of the relative coordinate kinetic energy (dot-dashed line), Ne-Ne potential energy (dotted line) and total relative energy (solid black line), during the formation of the Ne$_2$ molecule for $<v_0>$=120 m/s. The blue curve represents the evolution of $<r>$ and the red line refers to the projection of the vibrational wave function to the corresponding ground state vibrational wave function (i.e., $\left|\left\langle\varphi_{rel}|\varphi_{Ne_2(v=0)@\ ^4He_{500}}\right\rangle\right|^2(t)$; the y-axis range goes from 0 (low limit) up to 1(upper limit)). The first and third vertical lines show the first time that $<r>$ reaches the inner and outer turning points, respectively, and the second and fourth vertical lines show the two

first times where $<r>$ crosses the asymptotic $<r>$ value, once the $<r>$ vs time dependence presents an oscillating character.

Figure 7. Interaction potentials (Ne-Ne and Ne_2-helium and the sum of both terms) governing the Ne-Ne relative coordinate degree of freedom and the static (ground state (v=0)) relative coordinate wave packet (dashed line, black). The v=0 gas phase relative coordinate wave packet is shown in the red dashed line.

Figure 8. Energy per helium atom of the nanodroplet as a function of time. The inner panel focus on the initial part of the collision.

Figure 9. Number of helium atoms of the nanodroplet as a function of time.

Figures

Figure 1
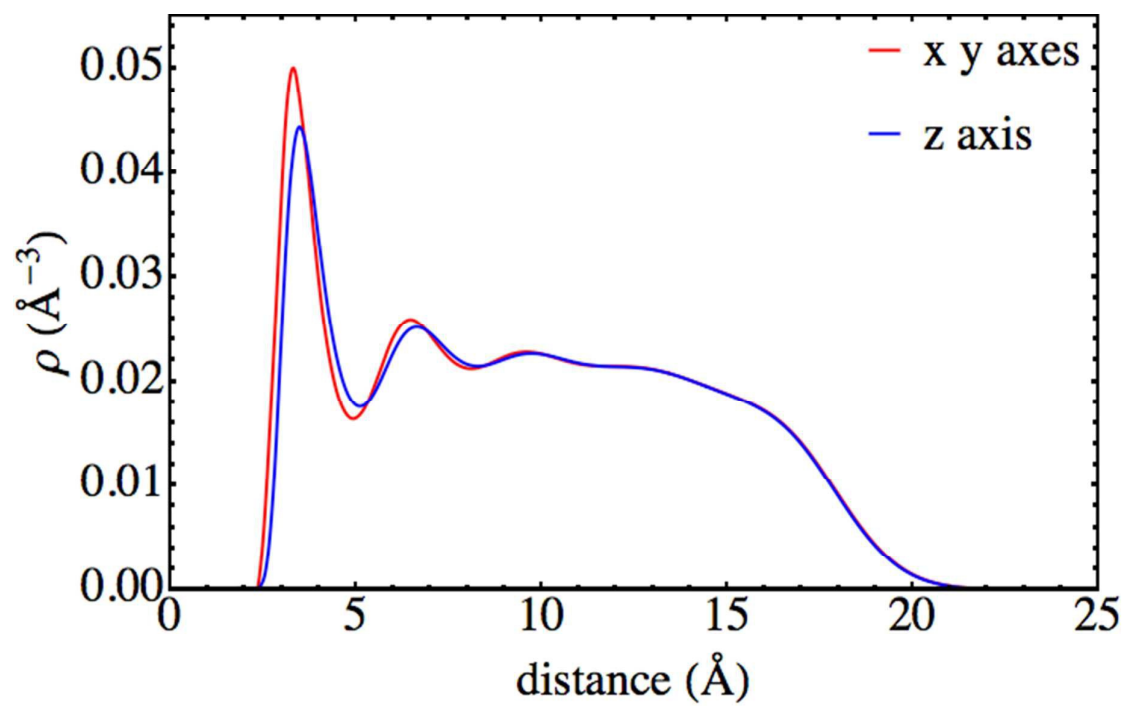
Figure 2
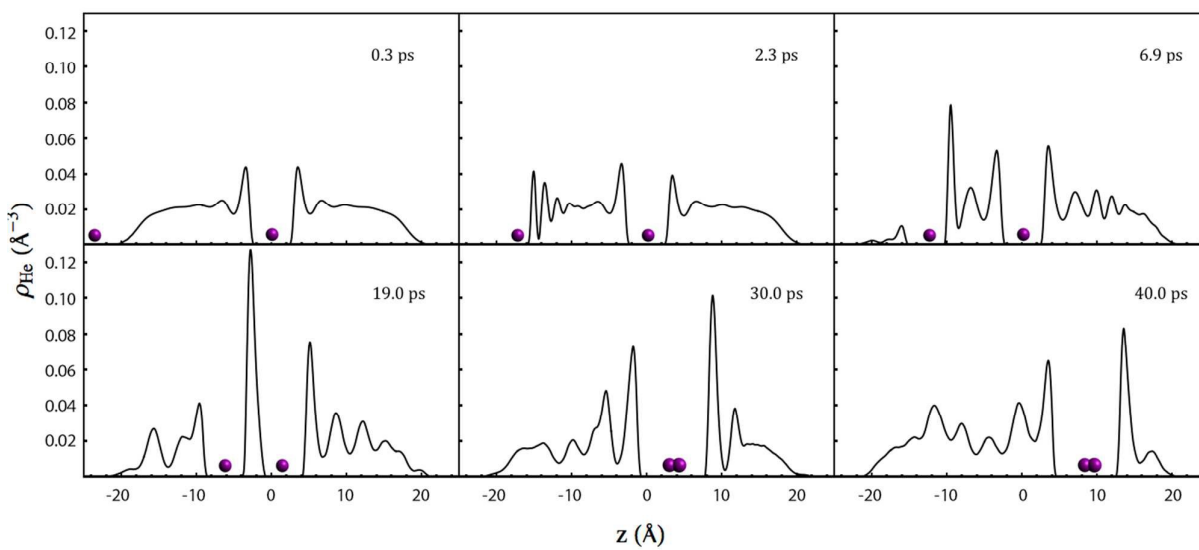
Figure 3
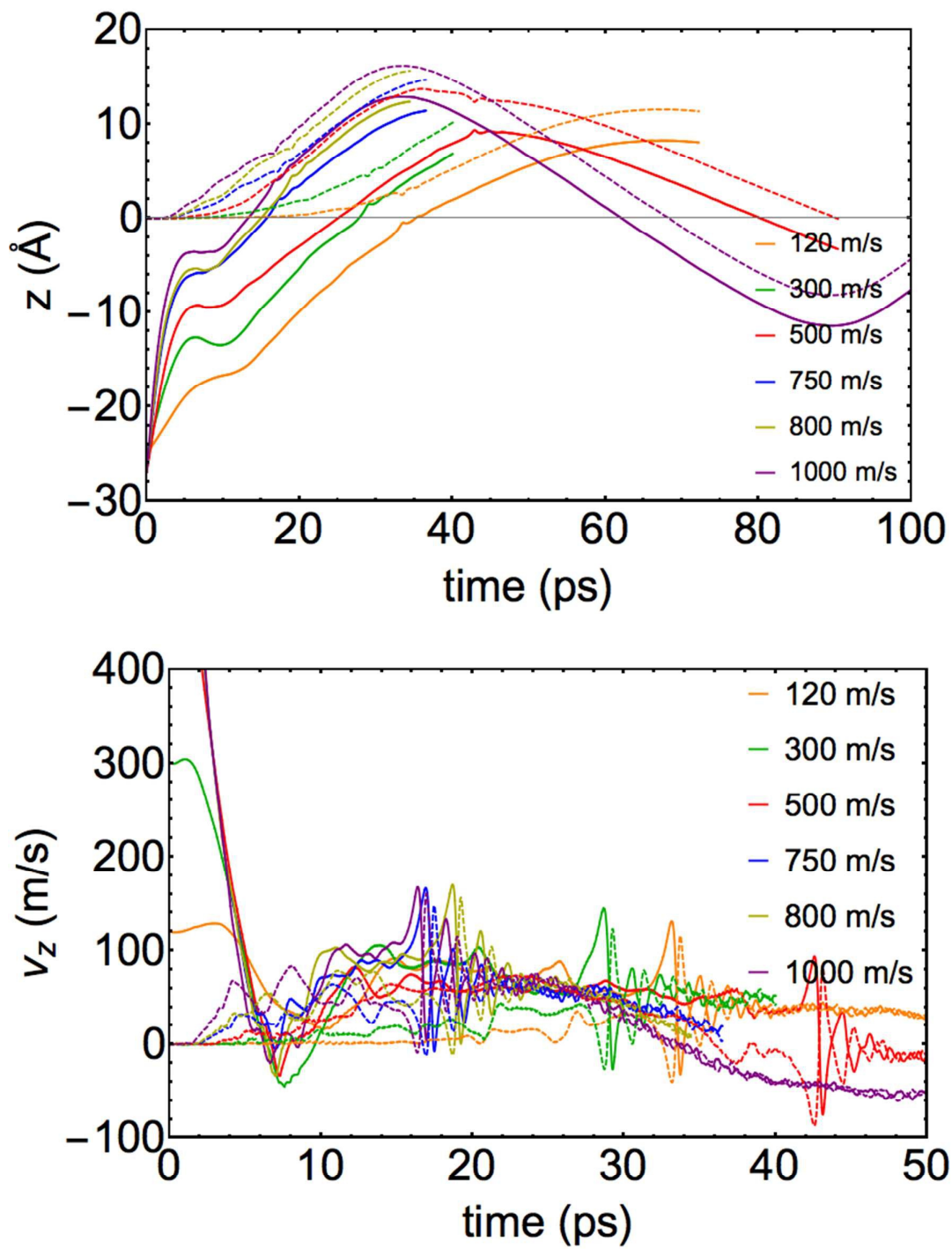
Figure 4
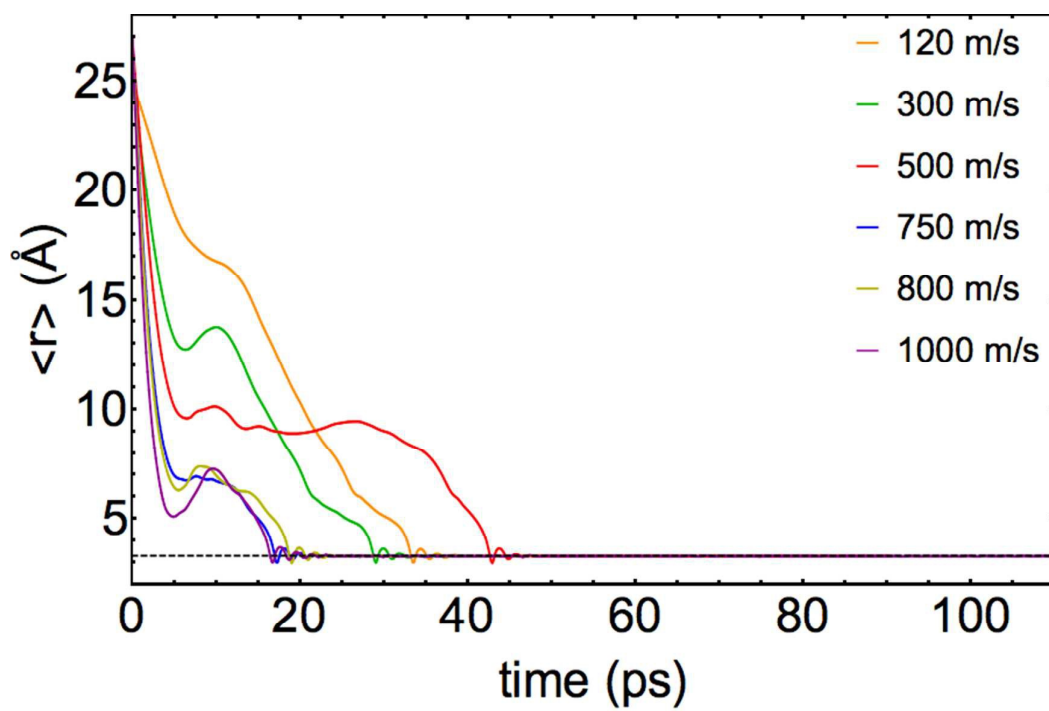
Figure 5
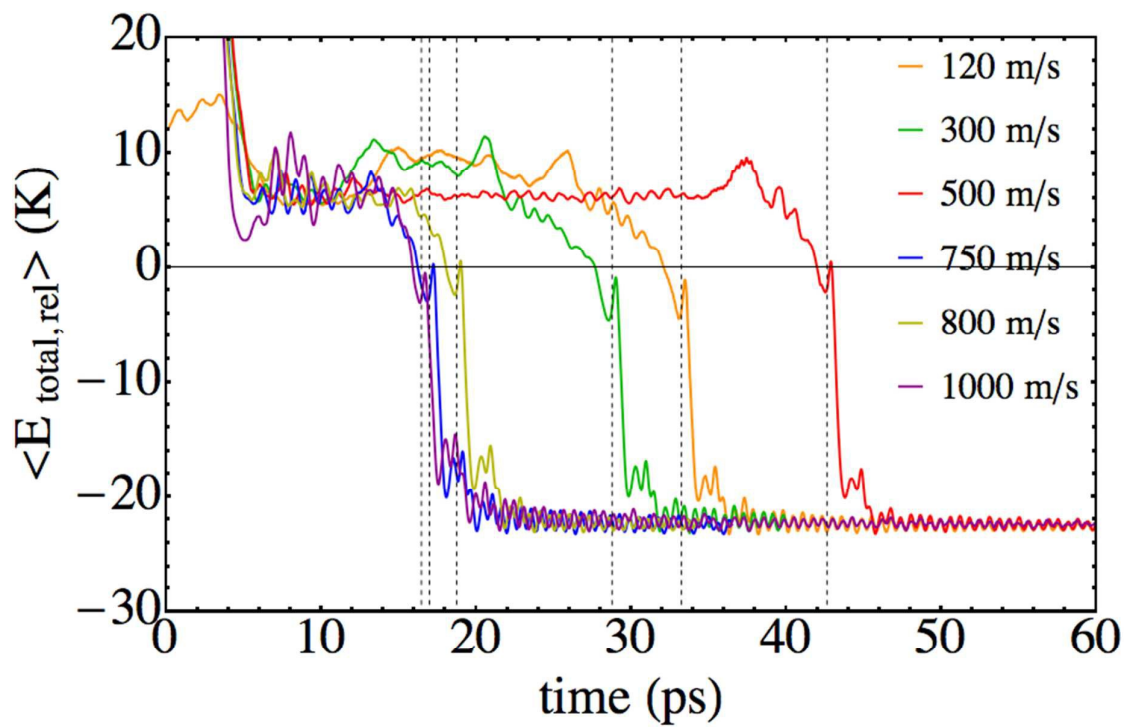
Figure 6
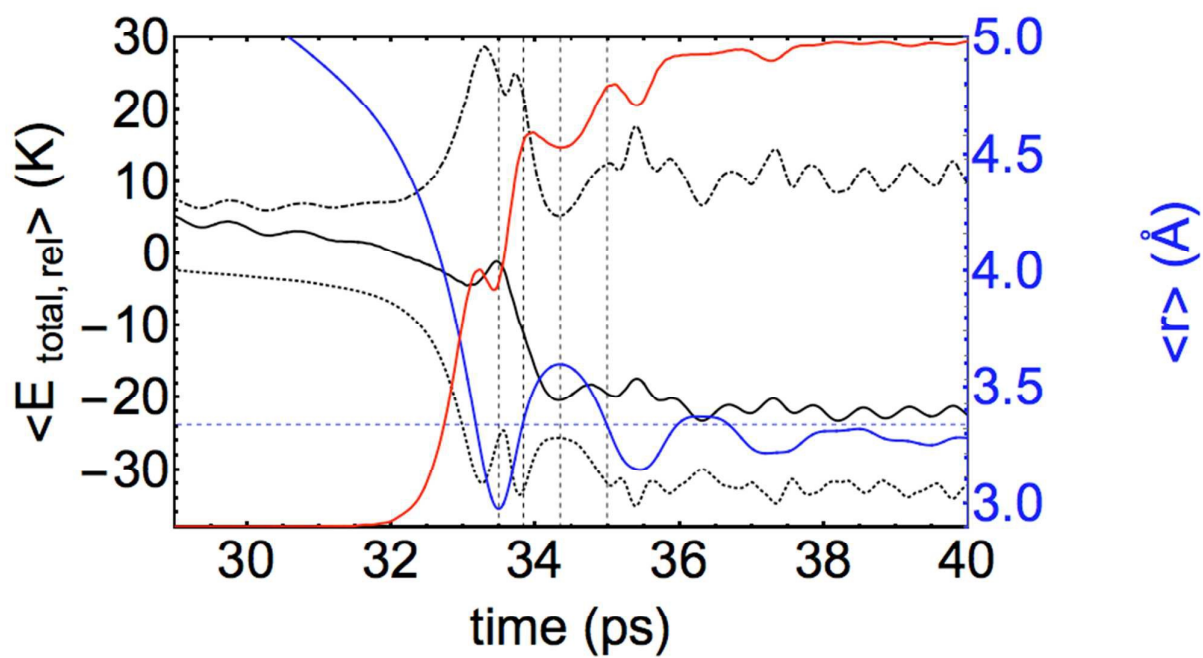
Figure 7
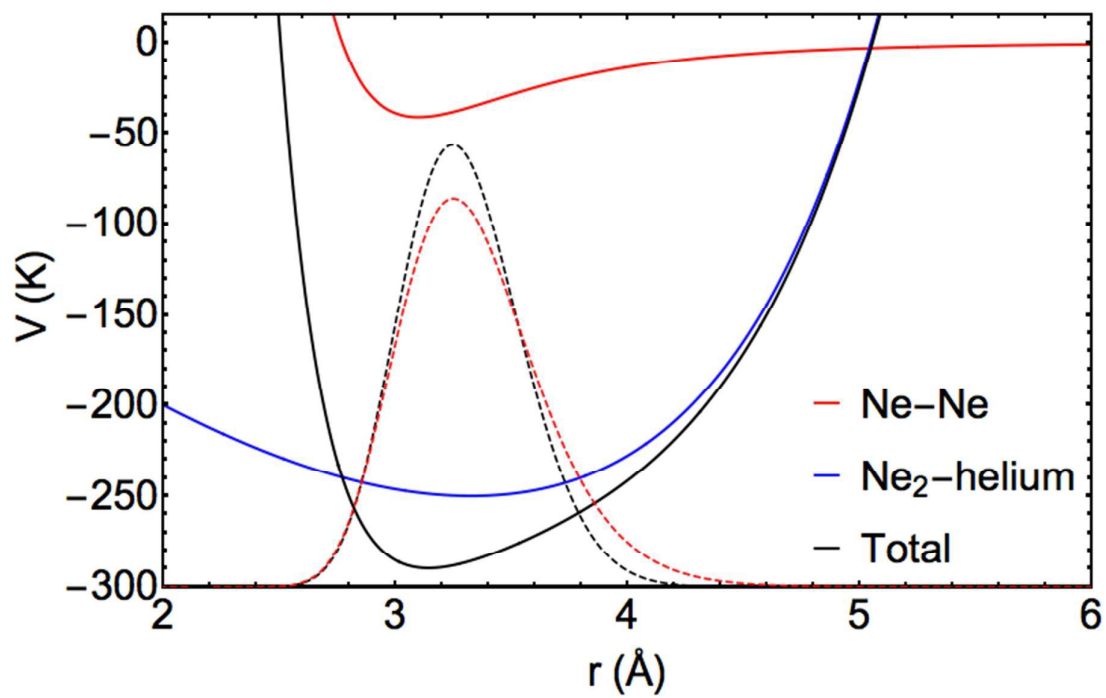
Figure 8
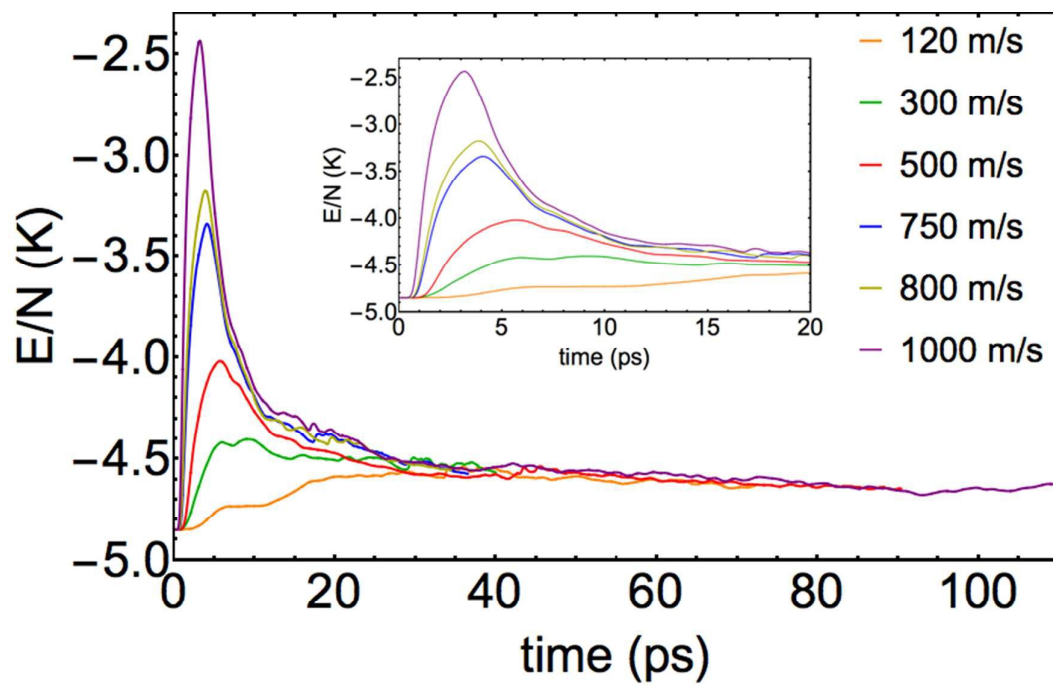
Figure 9
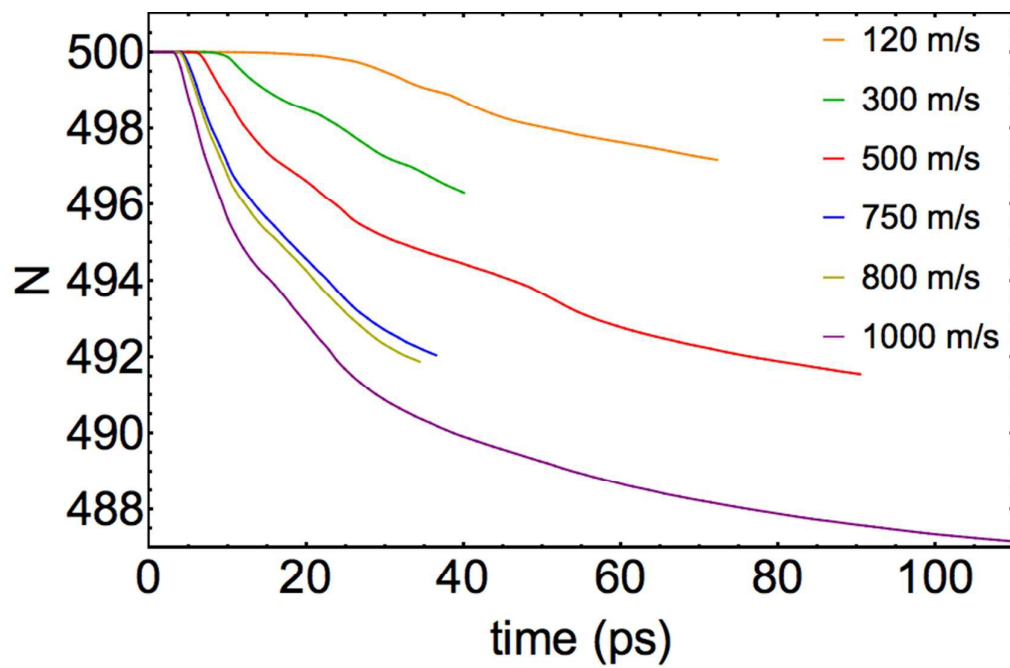
References

[1] J. P. Toennies and A. F. Vilesov, *Angew. Chem., Int. Ed.*, 2004, **43**, 2622.

[2] M. Barranco, R. Guardiola, S. Hernández, R. Mayol, J. Navarro and M. Pi, *J. Low Temp. Phys.*, 2006, **142**, 1.

[3] S. Goyal, D. L. Schutt and G. Scoles, *Phys. Rev. Lett.,* 1992, **69**, 933.

[4] M. Hartmann, R. E. Miller, J. P. Toennies and A. F. Vilesov, *Science*, 1996, **272**, 1631.

[5] A. Vilà, M. González, R. Mayol and M. Paniagua, *RSC Adv.*, 2014, **4**, 44972.

[6] A. Slenczka, and J. P. Toennies, in *Low Temperature and Cold Molecules*, ed. I. W. M. Smith, Imperial College Press, London, 2008, pp. 345-392 and references cited therein.

[7] S. Yang and A. M. Ellis, *Chem. Soc. Rev.*, 2013, **42**, 472.

[8] A. Vilà, M. González and R. Mayol, *J. Chem. Theory Comput.*, 2015, **11**, 899.

[9] A. Vilà, M. González and R. Mayol, *Phys. Chem. Chem. Phys.*, 2015, **17**, 32241.

[10] A. Vilà, M. González and R. Mayol, *Phys. Chem. Chem. Phys.*, 2016, **18**, 2409.

[11] A. Vilà, M. González and R. Mayol, *Phys. Chem. Chem. Phys.*, 2016, **18**, 2006.

[12] E. Lugovoj, J. P. Toennies and A. F. Vilesov, *J. Chem. Phys.*, 2000, **112**, 8217.

[13] G. E. Douberly and R. E. Miller, *J. Phys. Chem. B*, 2003, **107**, 4500.

[14] S. A. Krasnokutski and F. Huisken, *J. Phys. Chem. A.*, 2011, **115**, 7120.

[15] J. Tiggesbäumker and F. Stienkemeier, *Phys. Chem. Chem. Phys.*, 2007, **9**, 4748.

[16] T. Döppner, T. Diederich, S. Göde, A. Przystawik, J. Tiggesbäumker and K.-H. Meiwes-Broer, *J. Chem. Phys.*, 2007, **126**, 244513.

[17] S. Yang, A. M. Ellis, D. Spence, C. Feng, A. Boatwright, E. Latimer and C. Binns, *Nanoscale.* 2013, **5**, 11545.

[18] L. F. Gomez, E. Loginov and A. F. Vilesov, *Phys. Rev. Lett.*, 2012, **108**, 155302.

[19] E. Latimer, D. Spence, C. Feng, A. Boatwright, A. M. Ellis and S. Yang, *Nano Lett.*, 2014, **14**, 2902.

[20] A. Braun and M. Drabbels, *J. Chem. Phys.*, 2007, **127**, 114303.

[21] A. Braun and M. Drabbels, *J. Chem. Phys.*, 2007, **127**, 114304.

[22] A. Braun and M. Drabbels, *J. Chem. Phys.*, 2007, **127**, 114305.

[23] S. A. Krasnokutski and F. Huisken, *J. Phys. Chem. A*, 2010, **114**, 7292.

[24] T. Takayanagi and M. Shiga, *Chem. Phys. Lett.,* 2003, **372**, 90.

[25] G. Haberfehlner, P. Thaler, D. Knez, A. Volk, F. Hofer, W. E. Ernst and G. Kothleitner, *Nat. Commun.*, 2015, **6**, 8779.

[26] W. Hauser, A. Volk, P. Thaler and W. E. Ernst, *Phys. Chem. Chem. Phys.*, 2015, **17**, 10805.

[27] V. Mozhayskiy, M. N. Slipchenko, V. K. Adamchuk and A. F. Vilesov, *J. Chem. Phys.*, 2007, **127**, 094701.

[28] E. Loginov, L. F. Gomez and A. F. Vilesov, *J. Phys. Chem. A*, 2011, **115**, 7199.

[29] M. P. de Lara-Castells, N. F. Aguirre, H. Stoll, A. O. Mitrushchenkov, D. Mateo and M. Pi, *J. Chem. Phys.*, 2015, **142**, 131101.

[30] J. Eloranta, *Phys. Rev. B.,* 2008, **77**, 134301.

[31] J. Eloranta, *J. Low Temp. Phys.*, 2011, **162**, 718.

[32] D. Mateo, D. Jin, M. Barranco and M. Pi, *J. Chem. Phys.*, 2011, **134**, 044507.

[33] J. A. Martínez-González, M. González, L. Masgrau and R. Martínez, *ACS Catalysis*, 2015, **5**, 246.

[34] L. Giacomazzi, F. Toigo and F. Ancilotto, *Phys. Rev. B.,* 2003, **67**, 104501.

[35] D. Mateo, A. Hernando, M. Barranco, E. Loginov, M. Drabbels and M. Pi, *Phys. Chem. Chem. Phys.*, 2013, **15**, 18388.

[36] F. Dalfovo, L. Pricaupenko, S. Stringari and J. Treiner, *Phys. Rev. B*, 1995, **52**, 1193.

[37] N. B. Brauer, S. Smolarek, E. Loginov, D. Mateo, A. Hernando, M. Pi, M. Barranco, W. J. Bruma and M. Drabbels, *Phys. Rev. Lett.*, 2013, **111**, 153002.

[38] A. Leal, D. Mateo, A. Hernando, M. Pi and M. Barranco, *Phys. Chem. Chem. Phys.*, 2014, **16**, 23206.

[39] D. Mateo, F. Gonzalez and J. Eloranta, *J. Phys. Chem. A*, 2015, **119**, 2262.

[40] S. M. Cybulski and R. R. Toczylowski, *J. Chem. Phys.*, 1999, **111**, 10520.

[41] A. Ralston, in *Mathematical Methods for Digital Computers*, ed. A. Ralston and H. S. Wilf, John Wiley & Sons, New York, 1960, vol. 1, pp. 95-109.

[42] R. J. Thompson, *Commun. ACM.*, 1970, **13**, 739.

[43] M. Frigo and S. G. Johnson, *IEE Proc.*, 2005, **93**, 216.

[44] A. Vibók and G. G. Balint-Kurti, *J. Phys. Chem.*, 1992, **96**, 8712.

[45] D. R. Tilley and J. Tilley, *Condensates and Excitations. Superfluidity and Superconductivity*, Institut of Physics Publishing, Bristol, 1990, pp 41-53.

[46] J. F. Annet, *Superfluid Helium-4. Superconductivity, Superfluids and Condensates*, Oxford University Press, Oxford, 2004, pp 38-43.

[47] M. Lewerenz, B. Schilling and J. P. Toennies, *J. Chem. Phys.*, 1995, **102**, 8191.

[48] M. Lewerenz, B. Schilling and J. P. Toennies, *J. Chem. Phys.*, 1997, **106**, 5787.